# N-Methylation of diamino-substituted macrocyclic complexes: intramolecular cyclisation

**Paul V. Bernhardt,* Josephine C. Hetherington and Lathe A. Jones**

*Department of Chemistry, University of Queensland, Brisbane 4072, Australia*

Two new macropolycyclic hexaamines $L^2$ and $L^4$ as their copper(II) complexes have been isolated as products fro the condensation of the diamino-substituted macrocyclic complex *trans*-(6,13-dimethyl-1,4,8,11-tetraazacyclotetradecane-6,13-diamine)copper(II) $[CuL^1]^{2+}$ with aqueous formaldehyde. Both of the complexes exhibit methylene bridges between the pendant amine and the adjacent co-ordinated macrocyclic N-donors. Their crystal structures have been determined: $[CuL^2(NCS)][SCN]$, triclinic, space group $P\bar{1}$, $a = 7.133(2)$, $b = 9.813(2)$, $c = 16.745(3)$ Å, $\alpha = 101.05(2)$, $\beta = 99.36(2)$, $\gamma = 99.77(2)°$, $Z = 2$; $[CuL^4Cl][ClO_4]\cdot H_2O$, triclinic, space group $P\bar{1}$, $a = 9.3327(8)$, $b = 10.8989(6)$, $c = 12.672(1)$ Å, $\alpha = 68.591(6)$, $\beta = 78.899(6)$, $\gamma = 87.384(6)°$, $Z = 2$. The complexes exhibit square-pyramidal geometries, and significantly lower-energy electronic maxima relative to their parent complex $[CuL^1]^{2+}$. Electrochemistry of $[CuL^2]^{2+}$ revealed a reversible $Cu^{II}$-$Cu^{I}$ redox couple, by contrast to those of macromonocyclic analogues.

In the preceding paper[1] intermolecular reductive methylation of the primary amino groups appended to the macrocyclic complex $[CuL^1]^{2+}$ was achieved using the standard Eschweiler–Clarke ($CH_2O$–$HCO_2H$) procedure. In the course of that work an unexpected and unusual by-product was identified in low yield; namely the tetracyclic complex $[CuL^2]^{2+}$, in addition to the expected N-based isomers of $[CuL^3]^{2+}$. This observation prompted an investigation into the conditions under which inter- or intra-molecular condensation occurs in the reaction between formaldehyde and co-ordinated amines.

In this work two macropolycyclic complexes $[CuL^2]^{2+}$ and $[CuL^4]^{2+}$ have been synthesized, isolated and characterised both spectroscopically and by crystal structure analyses. A mechanism encompassing the formation of these two species as well as the macromonocyclic relatives $[CuL^3]^{2+}$ is presented, and the implications that these results have for other metal-directed template condensation reactions are discussed.

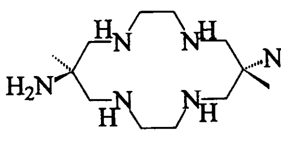
$L^1$

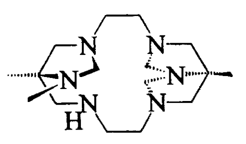
$L^2$

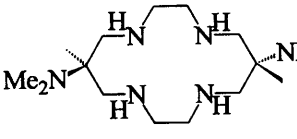
$L^3$

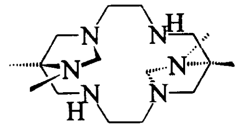
$L^4$

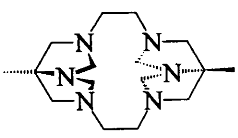
$L^5$

## Experimental

### Syntheses

*trans*-6,13-Dimethyl-1,4,8,11-tetraazacyclotetradecane-6,13-diamine hexahydrochloride ($L^1\cdot 6HCl$) was prepared as previously described.[2]

A purple solution of $Cu(NO_3)_2\cdot 2.5H_2O$ (0.94 g) and $L^1\cdot 6HCl$ (2.0 g) in water (10 $cm^3$) was prepared. Formaldehyde solution (20 $cm^3$, 32%) was added and the reaction mixture was refluxed for 24 h. It was diluted to 1 $dm^3$ and charged onto a 100 × 2 cm column of Sephadex C-25 cation exchange resin ($Na^+$ form). Elution with 0.05 mol $dm^{-3}$ trisodium citrate gave the following bands in the order: 1, blue-green, $Cu^{2+}(aq)$, which was discarded; 2 (see below); 3, purple, $\lambda_{max}$ 527 nm, β-$[CuL^1]^{2+}$, described elsewhere;[3] 4, purple, $\lambda_{max}$ 523 nm, α-$[CuL^1]^{2+}$, described elsewhere.[4]

**Band 2.** Indigo, $\lambda_{max}$ 554 nm, $[CuL^2]^{2+}/[CuL^4]^{2+}$. This solution was diluted ten-fold and charged on a Sephadex C-25 column (50 × 2 cm). Elution with 0.5 mol $dm^{-3}$ $NaClO_4$ solution afforded an intense indigo band which upon concentration yielded a purple powder of $[CuL^2][ClO_4]_2$ which was collected and washed with EtOH (0.6 g) (Found: C, 30.9; H, 5.8; N, 13.5. Calc. for $C_{16}H_{30}Cl_2CuN_6O_8\cdot 3H_2O$: C, 30.8; H, 5.7; N, 13.5%). Electronic spectrum (water): $\lambda_{max}$ 533 (ε 253) and 278 nm (6550 $dm^3$ $mol^{-1}$ $cm^{-1}$). Triangular shaped crystals of $[CuL^2(OH_2)][ClO_4]_2\cdot 2H_2O$ were obtained from later crops.† Blue crystals of $[CuL^2(NCS)][SCN]$ were grown by addition of an excess of NaSCN to an aqueous solution of $[CuL^2][ClO_4]_2$.

During the elution of $[CuL^2]^{2+}$ with 0.5 mol $dm^{-3}$ $NaClO_4$ as described above, a minor purple band precipitated at the top of the column. This compound redissolved and eluted when the eluent was changed to 0.5 mol $dm^{-3}$ NaCl. Concentration of the eluate to *ca.* 20 $cm^3$ afforded a precipitate of the mixed salt $[CuL^4Cl][ClO_4]\cdot 2H_2O$ on standing. The solid was filtered off and washed with ethanol (0.1 g). The second crop yielded purple crystals suitable for X-ray work (Found: C, 35.4; H, 6.7; N, 15.4. Calc. for $C_{16}H_{34}Cl_2CuN_6O_4\cdot 2H_2O$: C, 35.3; H, 7.0; N, 15.4%). Electronic spectrum (water): $\lambda_{max}$ 522 (ε 186) and 272 nm (7640 $dm^3$ $mol^{-1}$ $cm^{-1}$).

---

† Monoclinic space group, $P2_1$; *a* 9.62(1), *b* 13.699(9), *c* 10.168 Å, β 111.04(4)°. These crystals were twinned and the structure of $[CuL^2(OH_2)][ClO_4]_2\cdot 2H_2O$ could only be refined to an *R*1 of 0.13. However, the co-ordination geometry, ligand conformation and Cu–L bond lengths are not significantly different to those found in $[CuL^2(NCS)][SCN]$.

### Physical methods

Solution UV/VIS spectra were measured on a Perkin-Elmer Lambda 12 spectrophotometer. Cyclic voltammetry was performed with a BAS 100B analyser employing a glassy-carbon working electrode, an Ag–AgCl reference electrode and a platinum auxiliary electrode. All solutions were *ca.* $5 \times 10^{-3}$ mol dm$^{-3}$ in analyte and 0.1 mol dm$^{-3}$ in $NaClO_4$ and were purged with $N_2$ before measurement. Infrared spectra were measured on a Perkin-Elmer 1600 FT instrument. Molecular mechanics calculations were performed with the program MOMECPC[5] integrated with HYPERCHEM and employing a published force field.[6]

### Crystallography

**Crystal data.** $[CuL^2(NCS)][SCN]$. $C_{18}H_{32}CuN_8S_2$, $M = 488.2$, triclinic, space group $P\bar{1}$, $a = 7.133(2)$, $b = 9.813(2)$, $c = 16.745(3)$ Å, $\alpha = 101.05(2)$, $\beta = 99.36(2)$, $\gamma = 99.77(2)°$, $U = 1110.4(4)$ Å$^3$, $D_c$ $(Z = 2) = 1.460$ g cm$^{-3}$, $\mu$(Mo-K$\alpha$) = 11.94 cm$^{-1}$, $F(000) = 514$, $T = 293$ K. Specimen: purple needle $0.67 \times 0.17 \times 0.07$ mm, $A^*_{min,max}$ 1.00, 1.24; $N = 3908$, $N_o = 1751$ $[|F_o| > 2\sigma(|F_o|), 2 < \theta < 25°]$, *hkl* 0–8, −11 to 11, −19 to 19. Final $R1 = 0.071$, $wR2 = 0.131$, $w^{-1} = \sigma(F_o)^2 + (0.0538P)^2$ where $P = (F_o^2 + 2F_c^2)/3$, number of parameters = 262, goodness of fit = 1.015. Residual extrema +0.5, −0.6 e Å$^{-3}$.

$[CuL^4Cl][ClO_4]\cdot H_2O$. $C_{16}H_{36}Cl_2CuN_6O_5$, $M = 527.0$, triclinic, space group $P\bar{1}$, $a = 9.3327(8)$, $b = 10.8989(6)$, $c = 12.672(1)$ Å, $\alpha = 68.591(6)$, $\beta = 78.899(6)$, $\gamma = 87.384(6)°$, $U = 1177.1(2)$ Å$^3$, $D_c$ $(Z = 2) = 1.487$ g cm$^{-3}$, $\mu$(Mo-K$\alpha$) = 11.93 cm$^{-1}$, $F(000) = 554$, $T = 293$ K. Specimen: purple prism $0.30 \times 0.20 \times 0.20$ mm, $A^*_{min,max}$ 1.00, 1.12; $N = 4119$, $N_o = 2980$ $[|F_o| > 2\sigma(|F_o|), 2 < \theta < 25°]$, *hkl* 0–11, −12 to 12, −14 to 14. Final $R1 = 0.047$, $wR2 = 0.124$, $w^{-1} = \sigma(F_o)^2 + (0.0838P)^2 + 0.87P$ where $P = (F_o^2 + 2F_c^2)/3$, number of parameters = 410, goodness of fit = 1.023. Residual extreme + 0.7, −0.4 e Å$^{-3}$.

**Data collection.** Cell constants were determined by a least-squares fit to the setting parameters of 25 independent reflections measured on an Enraf-Nonius CAD4 four-circle diffractometer employing graphite-monochromated Mo-K$\alpha$ radiation (0.710 73 Å). For $[CuL^4Cl][ClO_4]\cdot H_2O$ the scan mode was $\omega$–2$\theta$ and for $[CuL^2(NCS)][SCN]$ the $\omega$ scan mode was used. Data reduction and absorption correction ($\psi$ scans) were performed with the XTAL package.[7]

**Structure solution.** Both structures were solved by heavy-atom methods with SHELXS 86[8] and refined by full-matrix least-squares analysis with SHELXL 93.[9] All non-H atoms were refined with anisotropic thermal parameters except the disordered O atoms in the structure of $[CuL^4Cl][ClO_4]\cdot H_2O$. The anion and solvent O atoms were refined with partial occupancies. Hydrogen atom positional and thermal parameters were refined in the structure of $[CuL^4Cl][ClO_4]\cdot H_2O$, but were fixed at estimated positions for the other structure. The atomic nomenclature is defined in Figs. 1 and 2 drawn with PLATON.[10]

Atomic coordinates, thermal parameters, and bond lengths and angles have been deposited at the Cambridge Crystallographic Data Centre (CCDC). See Instructions for Authors, *J. Chem. Soc., Dalton Trans.*, 1996, Issue 1. Any request to the CCDC for this material should quote the full literature citation and the reference number 186/260.

## Results

The tetracyclic complex $[CuL^2]^{2+}$ was obtained as a minor product of the standard $CH_2O$–$HCO_2H$ methylation procedure.[1] However, the yield of this compound was greatly enhanced by the omission of formic acid from the reaction. The same reaction also produced the tricyclic analogue $[CuL^4]^{2+}$ in low yield. In addition, unlike the standard $HCO_2H$–$CH_2O$ procedure, significant amounts of starting materials ($\alpha$- and $\beta$-$[CuL^1]^{2+}$) were recovered from the reaction mixture after work-up. The mechanistic implications of this result will be dealt with in the Discussion. Demetallation of $[CuL^2]^{2+}$, by Zn–HCl reduction of the metal centre results in decomposition of the ligand, to afford the mono-N-methylated derivative of $L^1$, where the three methylene linkages have been hydrolysed.

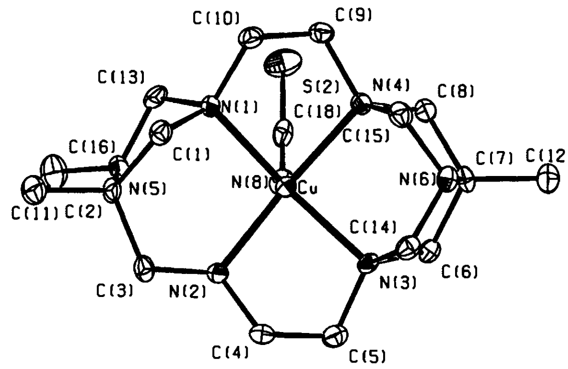

**Fig. 1** View of the $[CuL^2(NCS)]^+$ cation showing 20% probability ellipsoids (H atoms omitted for clarity)

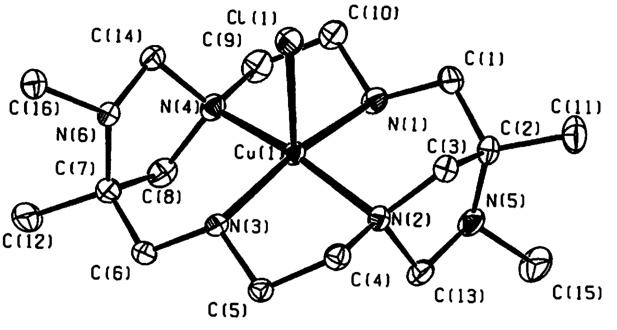

**Fig. 2** View of the $[CuL^4Cl]^+$ cation showing 20% probability ellipsoids (H atoms omitted for clarity)

The crystal structure analysis of $[CuL^2(NCS)][SCN]$ revealed all molecules on general sties. A view of the complex is shown in Fig. 1. Tetradentate co-ordination of the macrocycle is apparent with axial co-ordination of an isothiocyanate, resulting in a distorted square-pyramidal co-ordination sphere. The Cu atom is displaced from the $N_4$ plane by 0.28 Å towards the axial ligand. There is also a tetrahedral distortion of the four N-donors from the least-squares plane (0.05 Å). The co-ordinate bonds to the tertiary amines (Table 1) are somewhat longer than that to the secondary amine, but all macrocyclic Cu–N bond lengths are shorter than the axial Cu–NCS bond length. Three methylene bridges between the macrocyclic N atoms and the pendant amines are formed. The pairs of C–N bond lengths within these N–C–N links are significantly different, with the C–N bond further from the metal being the shorter (≈1.44 Å). This has also been found in other macrocyclic systems possessing the unusual, and generally unstable N–C–N group.[11,12] The single N-methyl C atom is oriented away from the complex. It is apparent that the structure of $[CuL^2(NCS)]^+$ is derived from the $\alpha$ isomer of $[CuL^1]^{2+}$, where the pendant amine and the two adjacent secondary amine H atoms are all *cis* with respect to each other as part of the same six-membered chelate ring. In this respect, the $\beta$ isomer of $[CuL^1]^+$ cannot be converted into $[CuL^2]^{2+}$ without N-inversion to $\alpha$-$[CuL^1]^{2+}$ taking place.

The crystal structure of $[CuL^4Cl][ClO_4]\cdot H_2O$ (Fig. 2) reveals a similar square-pyramidal co-ordination sphere, where a chloride occupies the axial co-ordination site. In this case, the pairs of *trans* Cu–N bond lengths are the same within experimental error (Table 2), the Cu–$NR_3$ bond lengths being longer than the pairs of Cu–$NHR_2$ bonds as expected. The Cu atom is displaced by 0.23 Å from the least-squares $N_4$ plane towards the axial chloride ligand, and a slight tetrahedral distortion (0.02

**Table 1** Bond lengths (Å) and angles (°) for $[CuL^2(NCS)]^+$

| | | | |
|---|---|---|---|
| Cu–N(2) | 2.018(6) | N(5)–C(13) | 1.44(1) |
| Cu–N(4) | 2.036(7) | N(5)–C(16) | 1.45(1) |
| Cu–N(3) | 2.038(6) | N(5)–C(2) | 1.47(1) |
| Cu–N(1) | 2.043(7) | N(6)–C(14) | 1.45(1) |
| Cu–N(8) | 2.196(8) | N(6)–C(15) | 1.46(1) |
| N(1)–C(1) | 1.48(1) | N(6)–C(7) | 1.50(1) |
| N(1)–C(10) | 1.49(1) | N(8)–C(18) | 1.17(1) |
| N(1)–C(13) | 1.49(1) | C(1)–C(2) | 1.54(1) |
| N(2)–C(4) | 1.48(1) | C(2)–C(11) | 1.52(1) |
| N(2)–C(3) | 1.48(1) | C(2)–C(3) | 1.54(1) |
| N(3)–C(5) | 1.46(1) | C(4)–C(5) | 1.51(1) |
| N(3)–C(6) | 1.48(1) | C(6)–C(7) | 1.54(1) |
| N(3)–C(14) | 1.50(1) | C(7)–C(12) | 1.52(1) |
| N(4)–C(9) | 1.469(9) | C(7)–C(8) | 1.54(1) |
| N(4)–C(8) | 1.48(1) | C(9)–C(10) | 1.51(1) |
| N(4)–C(15) | 1.52(1) | C(18)–S(2) | 1.64(1) |
| | | | |
| N(2)–Cu–N(4) | 166.9(3) | C(13)–N(5)–C(16) | 113.7(7) |
| N(2)–Cu–N(3) | 84.8(3) | C(13)–N(5)–C(2) | 108.3(7) |
| N(4)–Cu–N(3) | 90.1(3) | C(16)–N(5)–C(2) | 119.1(7) |
| N(2)–Cu–N(1) | 96.1(3) | C(14)–N(6)–C(15) | 113.3(7) |
| N(4)–Cu–N(1) | 84.7(3) | C(14)–N(6)–C(7) | 106.1(7) |
| N(3)–Cu–N(1) | 160.9(3) | C(15)–N(6)–C(7) | 106.4(6) |
| N(2)–Cu–N(8) | 98.8(3) | C(18)–N(8)–Cu | 133.1(7) |
| N(4)–Cu–N(8) | 94.0(3) | N(1)–C(1)–C(2) | 103.3(7) |
| N(3)–Cu–N(8) | 99.0(3) | N(5)–C(2)–C(11) | 116.3(7) |
| N(1)–Cu–N(8) | 99.8(3) | N(5)–C(2)–C(3) | 108.2(7) |
| C(1)–N(1)–C(10) | 112.5(7) | C(11)–C(2)–C(3) | 108.5(7) |
| C(1)–N(1)–C(13) | 99.5(6) | N(5)–C(2)–C(1) | 102.3(6) |
| C(10)–N(1)–C(13) | 115.4(6) | C(11)–C(2)–C(1) | 110.2(8) |
| C(1)–N(1)–Cu | 109.5(5) | C(3)–C(2)–C(1) | 111.2(7) |
| C(10)–N(1)–Cu | 108.4(5) | N(2)–C(3)–C(2) | 110.4(7) |
| C(13)–N(1)–Cu | 111.3(5) | N(2)–C(4)–C(5) | 107.9(7) |
| C(4)–N(2)–C(3) | 111.1(6) | N(3)–C(5)–C(4) | 108.6(7) |
| C(4)–N(2)–Cu | 107.5(5) | N(3)–C(6)–C(7) | 103.9(7) |
| C(3)–N(2)–Cu | 125.1(5) | N(6)–C(7)–C(12) | 113.5(7) |
| C(5)–N(3)–C(6) | 114.6(7) | N(6)–C(7)–C(8) | 103.7(7) |
| C(5)–N(3)–C(14) | 115.0(7) | C(12)–C(7)–C(8) | 113.2(7) |
| C(6)–N(3)–C(14) | 98.8(6) | N(6)–C(7)–C(6) | 103.3(6) |
| C(5)–N(3)–Cu | 107.6(5) | C(12)–C(7)–C(6) | 111.8(8) |
| C(6)–N(3)–Cu | 112.2(5) | C(8)–C(7)–C(6) | 110.6(7) |
| C(14)–N(3)–Cu | 108.3(5) | N(4)–C(8)–C(7) | 103.0(6) |
| C(9)–N(4)–C(8) | 113.8(6) | N(4)–C(9)–C(10) | 108.3(6) |
| C(9)–N(4)–C(15) | 115.2(7) | N(1)–C(10)–C(9) | 109.0(7) |
| C(8)–N(4)–C(15) | 98.8(6) | N(5)–C(13)–N(1) | 100.9(6) |
| C(9)–N(4)–Cu | 107.5(5) | N(6)–C(14)–N(3) | 104.7(7) |
| C(8)–N(4)–Cu | 114.7(5) | N(6)–C(15)–N(4) | 104.0(7) |
| C(15)–N(4)–Cu | 106.7(5) | N(8)–C(18)–S(2) | 178.2(9) |

**Table 2** Bond lengths (Å) and angles (°) for $[CuL^4Cl]^+$

| | | | |
|---|---|---|---|
| Cu–N(1) | 2.011(4) | N(5)–C(13) | 1.441(6) |
| Cu–N(3) | 2.031(4) | N(5)–C(15) | 1.454(7) |
| Cu–N(2) | 2.055(3) | N(5)–C(2) | 1.493(7) |
| Cu–N(4) | 2.064(4) | N(6)–C(14) | 1.434(6) |
| Cu–Cl(1) | 2.568(1) | N(6)–C(16) | 1.446(6) |
| N(1)–C(1) | 1.465(7) | N(6)–C(7) | 1.489(6) |
| N(1)–C(10) | 1.474(6) | C(1)–C(2) | 1.526(7) |
| N(2)–C(4) | 1.474(6) | C(2)–C(11) | 1.514(8) |
| N(2)–C(13) | 1.476(6) | C(2)–C(3) | 1.528(7) |
| N(2)–C(3) | 1.485(6) | C(4)–C(5) | 1.517(7) |
| N(3)–C(6) | 1.471(6) | C(6)–C(7) | 1.541(6) |
| N(3)–C(5) | 1.474(5) | C(7)–C(8) | 1.513(7) |
| N(4)–C(14) | 1.476(6) | C(7)–C(12) | 1.523(7) |
| N(4)–C(8) | 1.480(7) | C(9)–C(10) | 1.507(8) |
| N(4)–C(9) | 1.488(6) | | |
| | | | |
| N(1)–Cu–N(3) | 167.9(2) | C(13)–N(5)–C(15) | 113.0(5) |
| N(1)–Cu–N(2) | 92.1(2) | C(13)–N(5)–C(2) | 108.4(4) |
| N(3)–Cu–N(2) | 85.4(1) | C(15)–N(5)–C(2) | 119.4(5) |
| N(1)–Cu–N(4) | 85.1(2) | C(14)–N(6)–C(16) | 114.0(4) |
| N(3)–Cu–N(4) | 94.6(1) | C(14)–N(6)–C(7) | 107.9(4) |
| N(2)–Cu–N(4) | 166.1(1) | C(16)–N(6)–C(7) | 118.8(4) |
| N(1)–Cu–Cl(1) | 95.4(1) | N(1)–C(1)–C(2) | 111.2(4) |
| N(3)–Cu–Cl(1) | 96.5(1) | N(5)–C(2)–C(11) | 115.2(5) |
| N(2)–Cu–Cl(1) | 95.8(1) | N(5)–C(2)–C(1) | 107.7(4) |
| N(4)–Cu–Cl(1) | 98.0(1) | C(11)–C(2)–C(1) | 110.3(5) |
| C(1)–N(1)–C(10) | 114.0(4) | N(5)–C(2)–C(3) | 101.9(4) |
| C(1)–N(1)–Cu | 118.8(3) | C(11)–C(2)–C(3) | 110.3(5) |
| C(10)–N(1)–Cu | 106.0(3) | C(1)–C(2)–C(3) | 111.2(4) |
| C(4)–N(2)–C(13) | 114.4(4) | N(2)–C(3)–C(2) | 102.8(4) |
| C(4)–N(2)–C(3) | 113.5(4) | N(2)–C(4)–C(5) | 108.9(4) |
| C(13)–N(2)–C(3) | 100.0(4) | N(3)–C(5)–C(4) | 107.5(4) |
| C(4)–N(2)–Cu | 104.7(3) | N(3)–C(6)–C(7) | 112.1(4) |
| C(13)–N(2)–Cu | 112.4(3) | N(6)–C(7)–C(8) | 102.5(4) |
| C(3)–N(2)–Cu | 111.9(3) | N(6)–C(7)–C(12) | 115.0(4) |
| C(6)–N(3)–C(5) | 111.8(3) | C(8)–C(7)–C(12) | 110.9(5) |
| C(6)–N(3)–Cu | 122.4(3) | N(6)–C(7)–C(6) | 106.9(4) |
| C(5)–N(3)–Cu | 108.3(3) | C(8)–C(7)–C(6) | 111.5(4) |
| C(14)–N(4)–C(8) | 99.9(4) | C(12)–C(7)–C(6) | 110.0(5) |
| C(14)–N(4)–C(9) | 113.8(4) | N(4)–C(8)–C(7) | 103.8(4) |
| C(8)–N(4)–C(9) | 114.0(4) | N(4)–C(9)–C(10) | 110.1(4) |
| C(14)–N(4)–Cu | 112.9(3) | N(1)–C(10)–C(9) | 107.2(5) |
| C(8)–N(4)–Cu | 109.3(3) | N(5)–C(13)–N(2) | 103.9(4) |
| C(9)–N(4)–Cu | 107.0(3) | N(6)–C(14)–N(14) | 102.7(4) |

Å) of the macrocyclic donor atoms from the best plane is observed. The disordered perchlorate anion makes a weak contact [Cu· · ·O(3A) 3.55 Å] in the co-ordination site *trans* to the Cu–Cl bond. This distance is too large to be considered as a co-ordinate bond, so the complex ion is genuinely five-co-ordinate. The methylene bridges in the molecule $[CuL^4Cl]^+$ are derived from α-$[CuL^1]^{2+}$, and not from the N-based isomer β-$[CuL^1]^{2+}$.

The physical properties of $[CuL^2]^{2+}$ and $[CuL^4]^{2+}$ differ markedly from those of the monocyclic relatives α- and β-$[CuL^3]^{2+}$. The visible electronic maximum of $[CuL^2]^{2+}$ is found at lower energy relative to fourteen-membered tetraaza secondary amine analogues such as $[CuL^1]^{2+}$ and $[CuL^3]^{2+}$. The intensity of this transition is also *ca.* three times greater than that found in the centrosymmetric tetra-secondary amine parent complexes. The energy and intensity of the visible maximum of $[CuL^4]^{2+}$ is intermediate between those of α-$[CuL^3]^{2+}$ and $[CuL^2]^{2+}$. The shifts to lower energy of the visible maxima are a result of an extension of the Cu–N bond lengths relative to the parent secondary amine complexes, as well as a change in geometry from six- to five-co-ordinate.

Axial binding of a number of anionic ligands in the $[CuL^2(X)]^+$ system was investigated, where X = $F^-$, $Cl^-$, $Br^-$, $I^-$, $SCN^-$, $ClO_4^-$ or $CF_3SO_3^-$. Importantly, there was no significant variation in the absorption coefficient, which indicates that the co-ordination number remained the same throughout the series. However, the energy of the visible maximum was quite sensitive to the nature of the anion. It was found that the spectra measured in pure water, 1 mol $dm^{-3}$ $NaClO_4$, 1 mol $dm^{-3}$ $NaO_3SCF_3$ and 1 mol $dm^{-3}$ NaF each exhibited the same electronic energy maximum (≈533 nm) within experimental error. Therefore, it can be concluded that the actual species found in solution under these conditions is $[CuL^2(OH_2)]^{2+}$, as defined in the crystal structure analysis of $[CuL^2(OH_2)][ClO_4]_2{\cdot}2H_2O$. The spectra measured in 1 mol $dm^{-3}$ NaCl, 1 mol $dm^{-3}$ NaBr and 1 mol $dm^{-3}$ NaI all display electronic maxima around 547 nm. The most striking difference was found when the spectrum was measured in 1 mol $dm^{-3}$ NaSCN, where the maximum shifted to 570 nm (Fig. 3). Clearly, the $SCN^-$ ion is binding to the complex at this concentration ($[CuL^2]^{2+}:SCN^- \approx 1:1000$), and the crystal structure indicates that it is N-bound. The same shift in electronic maximum is seen in 1 : 20 mixtures of $[CuL^2][ClO_4]_2$ and NaSCN, which indicates that the equilibrium constant for the anation reaction (1) is considerable, relative to the

$$[CuL^2(OH_2)]^{2+} + SCN^- \rightleftharpoons [CuL^2(NCS)]^+ + H_2O \quad (1)$$

other anions investigated. No quantitative determinations of the anation equilibrium constants for these systems have been made at this time.

Cyclic voltammetry of $[CuL^2]^{2+}$ revealed a reversible $Cu^{II}$–$Cu^{I}$ couple at −0.872 V *vs.* Ag–AgCl. Reversibility was main-

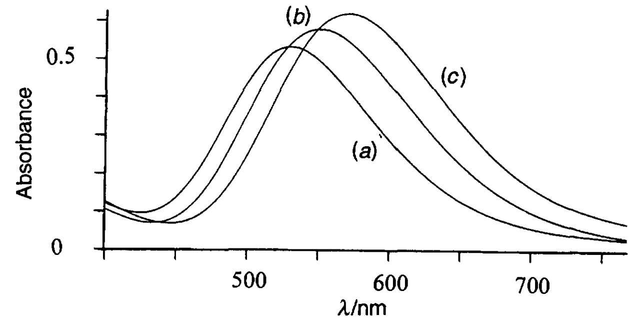

**Fig. 3** Visible electronic spectra of 2.0 × $10^{-3}$ mol $dm^{-3}$ solutions of $[CuL^2]^{2+}$ under the conditions: (*a*) 1 mol $dm^{-3}$ $NaClO_4$, (*b*) 1 mol $dm^{-3}$ NaCl and (*c*) 1 mol $dm^{-3}$ NaSCN

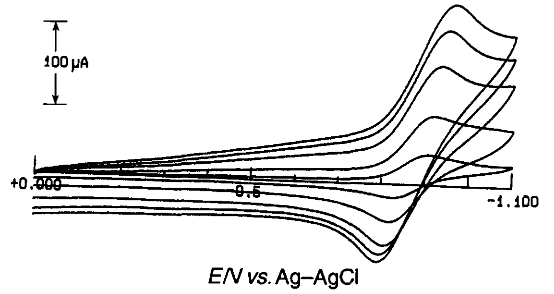

**Fig. 4** Cyclic voltammograms of $[CuL^2(OH_2)]^{2+}$ (glassy-carbon working electrode; 0.1 mol $dm^{-3}$ $NaClO_4$; scan rates 20, 100, 300, 500 and 700 mV $s^{-1}$)

tained ($i_a/i_c = 1.0$) at scan rates as low as 10 mV $s^{-1}$ (Fig. 4) indicating that the copper(I) complex is stable on the voltammetric time-scale; in this case at least 10 s. The anodic–cathodic peak separation increased slightly with scan rate which indicates that the rate of heterogeneous charge transfer becomes limiting at fast scan speeds. The voltammogram of $[CuL^4]^{2+}$ displayed an irreversible $Cu^{II}$–$Cu^{I}$ couple at *ca.* −0.90 V *vs.* Ag–AgCl, with only a weak, ill-defined anodic peak being observed. This behaviour is reminiscent of the typically irreversible $Cu^{II}$–$Cu^{I}$ couples found in tetraaza macromonocyclic complexes where rapid dissociation of the copper(I) complex occurs before reoxidation can occur.[1]

## Discussion

The results reported herein indicate that subtle variations to synthetic conditions can change the outcome of N-methylation reactions of $[CuL^1]^{2+}$. Omission of formic acid results in the dominant product being the tetracyclic $[CuL^2]^{2+}$, where intramolecular condensation is the major pathway. By contrast, inclusion of $HCO_2H$ affords copper(II) complexes of the bis(dimethylamino)-substituted macrocycle $L^3$ *via* a series of intermolecular reductive methylation steps. Methylene diamine (aminal) links such as those found in $[CuL^2(NCS)]^+$ and $[CuL^4Cl]^+$ are usually unstable, typically reverting to their parent aldehyde and amines.[13] However, it has been found that coordination by one of the amines in this group stabilises the aminal link,[14,15] and this has also been found with $[CuL^2]^{2+}$ and $[CuL^4]^{2+}$. Nevertheless, in all known cases, including this one, demetallation leads to immediate decomposition of these aminal groups.

These results highlight some interesting features concerning the mechanism of the Eschweiler[16]–Clarke[17] ($CH_2O$-$HCO_2H$) N-methylation procedure. The first step in the mechanism (with or without $HCO_2H$ present) involves a condensation between one $CH_2O$ molecule and a pendant primary amine, to generate a pendant methylene imine group (Scheme 1). The fate of this imine then largely determines the course of the reaction. One possibility is that (A) the imine is simply hydrolysed to the parent primary amine. The $CH_2O$–$RNH_2$ condensation is reversible and the significant amount of starting material recovered from the present reaction is a consequence of this. The second possibility is that the imine is reduced to an N-methyl group (B), as found in the $CH_2O$–$HCO_2H$ synthesis leading to $L^3$. It appears that formic acid plays an important (but not critical) role in facilitating the reduction step, as a succession of these steps leads almost exclusively to the N,N-dimethyl groups identified in the copper(II) complexes of $L^3$.

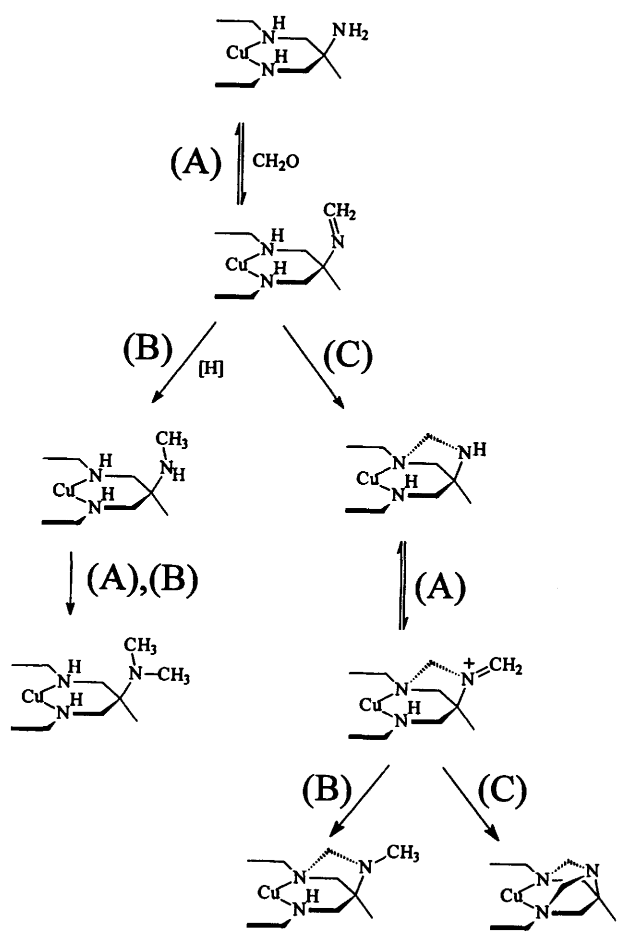

**Scheme 1**

The third outcome (C), is that the imine undergoes intramolecular nucleophilic attack by a neighbouring secondary amine to form an aminal (methylene diamine) link. This reaction is notable in that a nominally co-ordinated secondary amine can act as a nucleophile. The reaction is conducted in weakly acidic solution so there can be no way that the co-ordinated secondary amine might deprotonate to form a nucleophilic co-ordinated aminate group. Therefore, it is clear that nucleophilic addition occurs while the secondary amine is momentarily displaced from the metal, a prerequisite which is facilitated by the substitution labile copper(II) ion. This result has far reaching implications for other $Cu^{II}$-directed template condensations between co-ordinated amines and aldehydes, and implies that many of these reactions also take place while the amines are displaced from the metal. Direct evidence for this behaviour is very difficult to obtain because of the labile nature of these systems. Combinations of the three steps (A)–(C) account for all of the products observed in this work and the preceding paper.[1]

It is interesting that the N-methyl groups in $[CuL^2]^{2+}$ and $[CuL^4]^{2+}$ were formed in the absence of formic acid. That is, despite the fact that $HCO_2H$ greatly assists reduction to the N-methyl group, the acid itself is not the reducing species. Instead, $CH_2O$ must act as both the initial electrophile and also as the reductant in the present system. The relatively low yields of $[CuL^2]^{2+}$ and $[CuL^4]^{2+}$ compared with the amount of

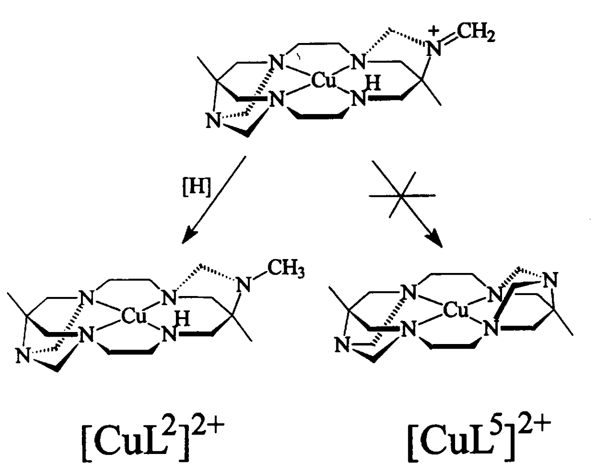

Scheme 2

recovered starting material indicates that the irreversible cyclisation step (C) is not competitive with the reversible condensation step (A) in the absence of $HCO_2H$, and the latter reaction simply regenerates the starting material. However, the irreversible reduction step (B) dominates both steps (A) and (C) when $HCO_2H$ is present. The fact that intramolecular cyclisation [step (C)] occurs at all is testimony to favourable entropy contributions which lead to typically rapid formation of five-membered rings. In this case cyclisation must occur during the brief time when there is a break in the secondary amine Cu–N bond coinciding with the presence of an adjacent methylene imine (or iminium) group.

The observation that only three intramolecular condensations occurred for $[CuL^2]^{2+}$ (and two for $[CuL^4]^{2+}$) poses the question as to why complete cyclisation to the copper(II) complex of the pentacyclic tertiary hexaamine $L^5$ was not found. Scheme 2 illustrates that this compound would have been formed if the final step in the synthesis of $[CuL^2]^{2+}$ had been an intramolecular condensation (C) instead of a reduction (B), but this was not observed. Despite the inherent complexities involved in the intramolecular reaction, the tetracyclic $[CuL^2]^{2+}$ was the major product of the reaction reported herein, whereas the tricyclic $[CuL^4]^{2+}$ ion was only isolated in very low yield. That is, step (B) is slow in the absence of $HCO_2H$, and the fused five- and six-membered ring 'football' structure is formed at one end of the molecule more rapidly than a terminating N-methylated, five-membered ring of the kind found in $[CuL^4]^{2+}$. Further condensation leads to the tetracyclic methylene iminium parent of $[CuL^2]^{2+}$ (Scheme 2). However, it seems that this molecule is unable to complete the final link between the only remaining secondary amine and this methylene iminium group, and ultimately the pendant imine is reduced to an N-methyl group to afford $[CuL^2]^{2+}$.

Molecular mechanics modelling of the as yet unobserved $[CuL^5(OH_2)]^{2+}$ complex was performed. The molecule is quite rigid, and only the five-membered chelate rings derived from the ethylenediamine residues possess conformational liability. Of the three non-degenerate conformers shown in Fig. 5 the isomer where the five-membered chelate rings are staggered [conformer (*b*)] is predicted to be at least 14 kJ mol$^{-1}$ more stable than the other two, and this would more than likely be the conformation in which it would be found. The predicted geometry displays shorter than usual Cu–N bond lengths for a tertiary amine[18,19] as well as a significant distortion towards trigonal-bipyramidal geometry: *trans* pairs of Cu–N bonds 1.995 and 2.045 Å, *trans* N–Cu–N 150.3 and 174.1°. The fact that the predicted Cu–N bond lengths in $[CuL^5(OH_2)]^{2+}$ are shorter than those of the observed analogues $[CuL^2(NCS)]^+$ and $[CuL^4Cl]^+$ indicates that the complex is quite strained within the rather small cavity defined by the ligand. Moreover, the calculated geometry suggests that the final intramolecular condensation step that is required to complete the pentacyclic structure of $[CuL^5(OH_2)]^{2+}$ will be difficult given the difference in Cu–N bond lengths between $[CuL^2(OH_2)]^{2+}$ (taken to represent the methylene iminium analogue in Scheme 2) and those predicted for $[CuL^5(OH_2)]^{2+}$. That is, the metal ion is probably too large to allow the methylene iminium group to approach the co-ordinated secondary amine such that intramolecular condensation can occur. Nevertheless, synthesis of this novel compound $L^5$ should be possible given the right templating conditions, probably involving a smaller metal ion.

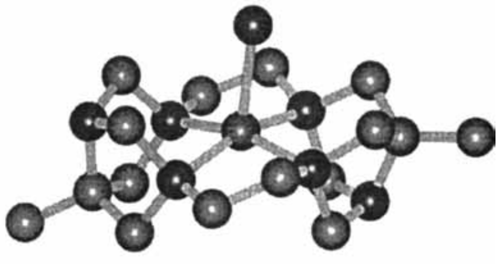

(*a*) 125.7 kJ mol$^{-1}$

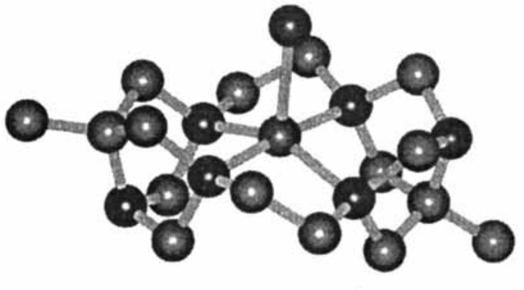

(*b*) 109.5 kJ mol$^{-1}$

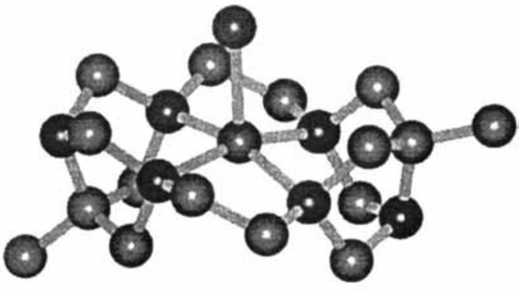

(*c*) 123.5 kJ mol$^{-1}$

**Fig. 5** Predicted strain-minimised geometries and energies of the three non-degenerate conformations of $[CuL^5(OH_2)]^{2+}$ (H atoms omitted for clarity)

The reversible electrochemical behaviour of $[CuL^2]^{2+}$ contrasts with the irreversible $Cu^{II}$–$Cu^{I}$ couples observed for α- and β-$[CuL^3]^{2+}$,[1] $[CuL^4]^{2+}$ and the parent complexes α- and β-$[CuL^1]^{2+}$.[3] Recent results have indicated that in-plane co-ordination of the Cu atom with respect to its four N-donors leads to rapid dissociation of the complex upon reduction to the monovalent state, in contrast to macrocyclic copper(II) complexes where the metal is displaced from the $N_4$ plane which typically lead to reversible $Cu^{II}$–$Cu^{I}$ waves, regardless of the type of N-donor, *e.g.* secondary or tertiary amine.[18,20] It is generally found that tertiary amines lead to an enhancement in the lifetime of copper(I) complexes relative to secondary and primary amine relatives. However, this may be a coincidence since tertiary amine complexes invariably exhibit greater distortions from ideal co-ordination geometries than secondary amine analogues as a result of the steric strain inherent to the sterically crowded tertiary amine donor atoms. In the rare cases where significant out-of-plane distortions have been effected on tetraaza macrocyclic secondary amine complexes, reversible electrochemical behaviour is found.[20]

The electronic spectroscopy of $[CuL^2(OH_2)]^{2+}$ indicated that the metal has quite a high affinity for axially bound anionic ligands. This property is not shared by tetragonally elongated six-co-ordinate relatives such as $[CuL^1]^{2+}$ and $[CuL^3]^{2+}$ where changes in their electronic spectrum are not nearly as great.[1,21] The greater sensitivity of five-co-ordinate copper(II) complexes to axial ligand co-ordination compared with six-co-ordinate analogues can be traced to the out-of-plane distortion that occurs going from a six- to a five-co-ordinate complex. Strong axial binding draws the metal centre further from the basal $N_4$ plane in square-pyramidal complexes, which results in both an extension of the macrocyclic Cu–N bond lengths as well as misalignment of the donor atoms with respect to the metal d orbitals. An alternative view is that the metal is already displaced from the macrocyclic plane by virtue of the strained ligand conformation, and its Lewis acidity is enhanced through a weakening of the bonding interaction with the macrocyclic N-donors.

By contrast, co-ordination by pairs of ligands in *trans* sites of a six-co-ordinate complex does not result in a net out-of-plane distortion, as the influence of each axially bound ligand opposes the other, and the metal remains in the centre of the macrocycle. As a consequence, bathochromic shifts in the visible electronic maxima of five-co-ordinate copper(II) complexes relative to six-co-ordinate analogues are invariably found.

## Conclusion

Intramolecular condensation reactions of formaldehyde with the diamino-substituted macrocyclic complex $[CuL^1]^{2+}$ can be achieved by inhibiting competing reduction steps which lead to N-methylation. It was found that formic acid facilitates the N-methylation reaction, and its omission from the reaction mixture has allowed the synthesis of the two novel polycyclic compounds $L^2$ and $L^4$ as their copper(II) complexes. The fused five- and six-membered ring moiety found in $L^2$ represents a new type of structurally reinforced macrocycle. The enhanced reversibility of the electrochemical reduction of $[CuL^2]^{2+}$ relative to macromonocyclic analogues illustrates the unique properties of tertiary amine complexes, and further studies with reactions of this type are continuing.

## Acknowledgements

Financial support from the University of Queensland and the Energy Research and Development Corporation is gratefully acknowledged.

## References

1 P. V. Bernhardt, *J. Chem. Soc., Dalton Trans.*, preceding paper.

2 P. V. Bernhardt, P. Comba, T. W. Hambley, G. A. Lawrance and K. Várnagy, *J. Chem. Soc., Dalton Trans.*, 1992, 355.

3 P. Comba, N. F. Curtis, G. A. Lawrance, A. M. Sargeson, B. W. Skelton and A. H. White, *Inorg. Chem.*, 1986, **25**, 4260.

4 G. A. Lawrance, B. W. Skelton, A. H. White and P. Comba, *Aust. J. Chem.*, 1986, **39**, 1101.

5 P. Comba and T. W. Hambley, MOMECPC, A Molecular Mechanics Program for Coordination Compounds,Universities of Heidelberg and Sydney, 1995.

6 P. V. Bernhardt and P. Comba, *Inorg. Chem.*, 1992, **31**, 2638.

7 S. R. Hall, H. D. Flack and J. M. Stewart (Editors), *The XTAL3.2 User's Manual*, Universities of Western Australia, Geneva and Maryland, 1992.

8 G. M. Sheldrick, *Acta Crystallogr., Sect. A*, 1990, **46**, 467.

9 G. M. Sheldrick, SHELXL 93, Program for Crystal Structure Determination, University of Göttingen, 1993.

10 A. L. Spek, *Acta Crystallogr., Sect. A*, 1990, **46**, C34.

11 I. I. Creaser, R. J. Geue, J. M. Harrowfield, A. J. Herlt, A. M. Sargeson, M. R. Snow and J. Springborg, *J. Am. Chem. Soc.*, 1982, **104**, 6016.

12 M. P. Suh, B. Y. Shim and T.-S. Yoon, *Inorg. Chem.*, 1994, **33**, 5509.

13 J. March, *Advanced Organic Chemistry*, Wiley-Interscience, New York, 1992.

14 M. P. Suh, W. Shin, H. Kim and C. H. Koo, *Inorg. Chem.*, 1987, **26**, 1846.

15 L. Fabbrizzi, A. M. Mannotti Lanfredi, P. Pallavicini, A. Perotti, A. Taglietti and F. Ugozzoli, *J. Chem. Soc., Dalton Trans.*, 1991, 3263.

16 W. Eschweiler, *Chem. Ber.*, 1905, **38**, 880.

17 H. T. Clarke, H. B. Gillespie and S. Z. Weishaus, *J. Am. Chem. Soc.*, 1933, **55**, 4571.

18 P. V. Bernhardt, J. M. Harrowfield, D. C. R. Hockless and A. M. Sargeson, *Inorg. Chem.*, 1994, **33**, 5659.

19 T.-J. Lee, T.-Y. Lee, C.-Y. Hong, D.-F. Wu and C.-S. Chung, *Acta Crystallogr., Sect. C*, 1986, **42**, 999.

20 P. V. Bernhardt and P. C. Sharpe, *Chem. Commun.*, 1996, 1267.

21 P. V. Bernhardt, unpublished work.

*Received* 11*th June* 1996; *Paper* 6/04117E